INVESTIGATION OF ORDER OF ACCURACY FOR HIGHER ORDER FINITE VOLUME SCHEMES[1]

Vít Dolejší and Jiří Felcman
Faculty of Mathematics and Physics
Charles University Prague
Malostranské nám. 25
118 00 Praha 1, Czech Republic

Abstract

The paper is concerned with the higher order extension of the cell centred finite volume scheme for the numerical modelling of inviscid gas flow. In the smooth part of the flow field, first order accuracy is not accurate enough. Furthermore, the shocks and contact discontinuities are smeared out because of the numerical viscosity hidden in the first order scheme. Therefore, we wish to improve the order of accuracy on one hand and to resolve discontinuities without introducing over or undershoots on the other hand. In the last several years there has been considerable effort aimed at constructing and analyzing high order accurate, non-oscillatory approximations to hyperbolic conservation laws. Here we investigate several methods and determine the order of accuracy for Sod's channel where the analytical solution is known. The computation is performed for three different triangulations with sizes of mesh h, $h/2$ and $h/4$ and the determination of the order of accuracy is done using the method of the least squares.

Keywords: compressible flow, Euler equations, finite volume method, upwind flux vector splitting schemes of Godunov type, higher order method

1 Formulation of Problem

We consider the first order hyperbolic system in a space-time cylinder $Q_T = \Omega \times (0, T)$

$$\frac{\partial w}{\partial t} + \sum_{s=1}^{2} \frac{\partial f_s(w)}{\partial x_s} = 0 \tag{1}$$

describing the inviscid compressible flow. Here

$$\begin{aligned} &w = (\rho,\, \rho v_1,\, \rho v_2,\, e)^T, \quad w = w(x,t), \quad x \in \Omega, \quad t \in (0,T), \\ &f_s(w) = (\rho v_s,\, \rho v_s v_1 + \delta_{s1} p,\, \rho v_s v_2 + \delta_{s2} p,\, (e+p)\, v_s)^T \end{aligned} \tag{2}$$

and p is given by the state equation

$$p = (\gamma - 1)\,(e - \rho|\boldsymbol{v}|^2/2).$$

We use the standard notation: t – time, x_s $(s = 1, 2)$ – Cartesian coordinates, ρ – density, p – pressure, e – total energy, $\boldsymbol{v} = (v_1, v_2)$ – velocity, δ_{ij} – Kronecker delta, $\gamma > 1$ is the Poisson adiabatic constant.

The initial condition and a set of boundary conditions complete the above system. For their description see e. g. [3].

[1]This work was supported under the grant No. 201/96/0313 of the Czech Grant Agency.

Let the domain Ω be approximated by a polygonal domain Ω_h. We construct a triangulation $\mathcal{D}_h$ of Ω_h with the usual properties (in the sense of the finite element method), $\mathcal{D}_h = \{D_i\}_{i\in I}$, I is a suitable index set. We denote by h the mesh size parameter, i.e.

$$h = \max_{D_i \in \mathcal{D}_h} \mathrm{diam} D_i. \tag{3}$$

The boundary ∂D_i of the triangle D_i can be expressed in the form

$$\partial D_i = \bigcup_{j \in S(i)} \Gamma_{ij}, \tag{4}$$

where Γ_{ij} is either the common side of two neighbouring triangles D_i and D_j or $\Gamma_{ij} \subset \partial\Omega_h$. $S(i)$ is an index set. Furthermore, we introduce the following notation: $|D_i|$ = area of D_i, $n_{ij} = (n_1, n_2)$ = unit outer normal to ∂D_i on Γ_{ij}, ℓ_{ij} = length of Γ_{ij}, $0 = t_0 < t_1 < \dots$ is a partition of the time interval $(0, T)$ and $\tau_k = t_{t+1} - t_k$ is a time step, $k = 0, 1, \dots$.

The *finite volume (cell centred) discretization* is based on the integration of (1) over every set $D_i \times (t_k, t_{k+1})$, the use of Green's theorem, the approximation of the exact solution w averaged at time t_k over the triangle D_i by constant values w_i^k and the approximation of the flux

$$\int_{\Gamma_{ij}} \sum_{s=1}^{2} f_s(w)\, n_s \;\, dS$$

of the quantity w through the segment Γ_{ij} in the direction n_{ij} per second on the time level t_k with the aid of the so-called *numerical flux* $H(w_i^k, w_j^k, n_{ij})$ calculated from w_i^k, w_j^k and n_{ij}. In this way we obtain the following explicit numerical scheme:

$$\begin{aligned} w_i^{k+1} &= w_i^k - \frac{\tau_k}{|D_i|} \sum_{j \in S(i)} H(w_i^k, w_j^k, n_{ij})\, \ell_{ij}, \\ &\qquad\qquad D_i \in \mathcal{D}_h \ (\text{i.e., } i \in I),\ k = 0, 1, \dots . \end{aligned} \tag{5}$$

In case that $\Gamma_{ij} \subset \partial\Omega_h$, it is necessary to determine the boundary state on Γ_{ij}. For the evaluation of the numerical flux in (5) the *Osher–Solomon scheme* is used (see [6]).

2 Higher Order Reconstruction

The higher order extension of the scheme (5) lies in the nature of the preprocessing of the cell averaged data, which is accomplished via a nearest neighbour linear interpolation followed by a slope limiting procedure. The numerical flux $H(w_i^k, w_j^k, n_{ij})$ in the scheme (5) (this scheme is denoted as BASIC) is replaced by the flux $H(\hat{w}_{ij}^k, \hat{w}_{ji}^k, n_{ij})$, where values $\hat{w}_{ij}^k$, $\hat{w}_{ji}^k$ are reconstructed component-wise from the cell averaged data in the following form

$$\hat{w}_{ij}^k = w_i^k + \nabla L_i \cdot (x_i - x_{ij}, y_i - y_{ij})^T, \quad i \in I, j \in S(i). \tag{6}$$

Here (x_i, y_i) is the center of gravity of D_i, (x_{ij}, y_{ij}) is the center of Γ_{ij} and L_i is a linear function defined on $D_i \in \mathcal{D}_h$ (see Figure 1). We call L_i a linear reconstruction of w on D_i. We have proposed and tested several different methods and completed them by the comparison with the results from [2, 5]. For all of this methods the order of accuracy is numerically determined and methods are mutually compared. Now we describe the computation of L_i for each of tested methods (we omit the "time" index k).

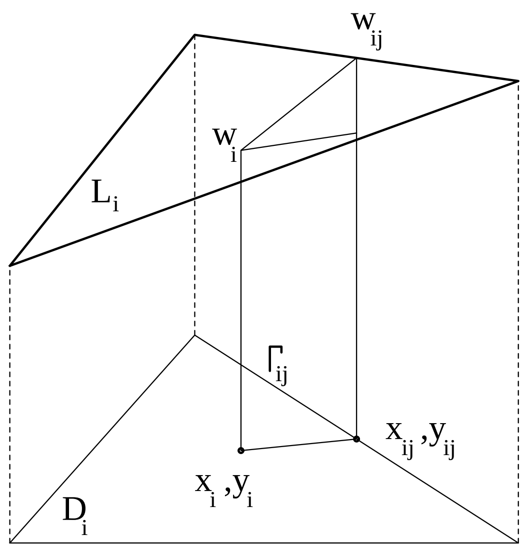

Figure 1: Linear reconstruction on D_i

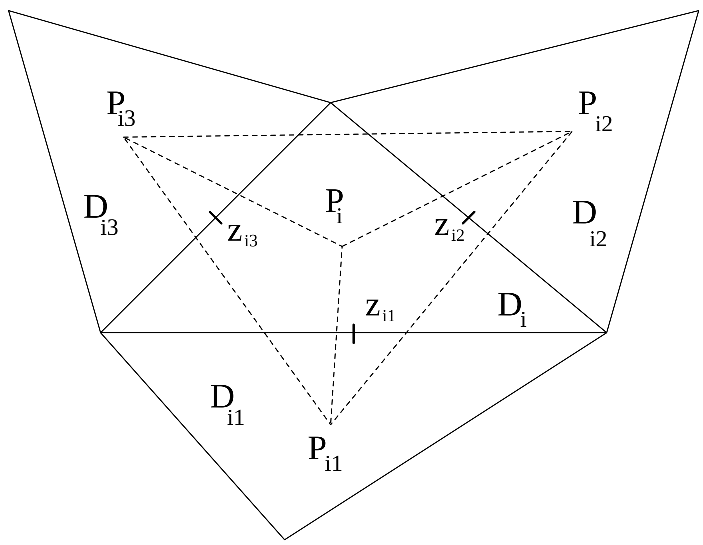

Figure 2: Triangle D_i and its neighbours D_{i1}, D_{i2}, D_{i3}, corresponding centers of gravity $P_i, P_{i1}, P_{i2}, P_{i3}$ and centers z_1, z_2, z_3 of edges of D_i.

2.1 Description of Higher Order Schemes

1. **DEO–M**. This method was proposed in [2]. We associate the value of w_i with the center of gravity of D_i. For each finite volume $D_i \in \mathcal{D}_h$, $D_i \cap \partial\Omega_h = \emptyset$, there exist three neighbouring triangles: D_{i1}, D_{i2}, D_{i3}. Let D_{i1}, D_{i2}, D_{i3} be the neighbours of D_i and $w_i, w_{i1}, w_{i2}, w_{i3}$ the corresponding values of the approximate solution. By $P_i, P_{i1}, P_{i2}, P_{i3}$ we denote the centers of gravity of $D_i, D_{i1}, D_{i2}, D_{i3}$, respectively. The centers of edges of D_i are denoted by z_{i1}, z_{i2}, z_{i3} (see Figure 2). There exist linear functions L_{i1}, L_{i2}, L_{i3} such that

$$\begin{array}{lll} L_{i1}(P_i) = w_i, & L_{i1}(P_{i1}) = w_{i1}, & L_{i1}(P_{i2}) = w_{i2}, \\ L_{i2}(P_i) = w_i, & L_{i2}(P_{i2}) = w_{i2}, & L_{i2}(P_{i3}) = w_{i3}, \\ L_{i3}(P_i) = w_i, & L_{i3}(P_{i3}) = w_{i3}, & L_{i3}(P_{i1}) = w_{i1}. \end{array} \tag{7}$$

   We put

$$|L_{ij}| := \left[\left(\frac{\partial L_{ij}}{\partial x_1} \right)^2 + \left(\frac{\partial L_{ij}}{\partial x_2} \right)^2 \right]^{\frac{1}{2}}. \tag{8}$$

   The following procedure for construction of L_i is used:

   (a) We reorder (using a permutation) $L_{ij},\ j = 1,2,3$ onto $L^{ij},\ j = 1,2,3$ such that $|L^{i1}| \geq |L^{i2}| \geq |L^{i3}|$ and set $L_i := L^{i1}$.

   (b) We verify the following conditions

$$\begin{array}{l} L_i(z_{i1}) \text{ is between } w_i \text{ and } w_{i1}, \\ L_i(z_{i2}) \text{ is between } w_i \text{ and } w_{i2}, \\ L_i(z_{i3}) \text{ is between } w_i \text{ and } w_{i3}. \end{array} \tag{9}$$

   If all conditions (9) are satisfied then the procedure is finished. If this is not the case we continue to the next step.

   (c) We put $L_i := L_{i2}$ and we test the condition (9) again. If the conditions (9) are satisfied for the second candidate we take it, if not we set $L_i := L^{i3}$ and finish the procedure , i.e. for the L^{i3} conditions (9) are not tested.

2. **DEO–B**. This method is very similar to DEO-M. The condition (9) are tested also for the case when we chose $L_i := L^{i3}$. If L^{i3} does not satisfy the conditions (9) then we put $L_i := 0$, i.e. we use $\hat{w}_{ij} = w_i$.

3. **MIN**. Also this method is a modification of **DEO–M**. We put directly $L_i := L^{i3}$, i.e. from three candidates we choose this one whose absolute value of the gradient is minimal. This construction is analogous to ENO-schemes.

4. **AVER**. The weighted average of three linear functions is chosen. Using the previous notation we set

$$L_i := \frac{L_{i1}|P_iP_{i1}P_{i2}| + L_{i2}|P_iP_{i2}P_{i3}| + L_{i3}|P_iP_{i3}P_{i1}|}{|P_iP_{i1}P_{i2}| + |P_iP_{i2}P_{i3}| + |P_iP_{i3}P_{i1}|}, \tag{10}$$

   where $|P_iP_{i1}P_{i2}|$ is the area of triangle $P_iP_{i1}P_{i2}$ and similarly for triangles $P_iP_{i2}P_{i3}$ and $P_iP_{i3}P_{i1}$.

5. **EXTRAP**. In order to involve more information into the scheme, we extrapolate cell average values into vertices and construct their linear interpolant. Let $D_i \in \mathcal{D}_h$ and $X_{i_1}, X_{i_2}, X_{i_3}$ be the vertexes of D_i. For each X_{i_j}, $j = 1,2,3$, $i \in J$ (= an index set of all nodes from $\mathcal{D}_h$) we define a set $Y(X_{i_j}) = \{k \in I;\ X_{i_j}$ is a vertex of $D_k\}$. Then we extrapolate the cell data into the vertices X_{i_j}, $j = 1,2,3$, $i \in J$ setting

$$\bar{w}(X_{i_j}) = \frac{\sum_{k \in Y(X_{i_j})} w_k |D_k|}{\sum_{k \in Y(X_{i_j})} |D_k|}, \tag{11}$$

where $|D_k|$ denotes the area of D_k. Now we construct a linear function L_i, $i \in I$ satisfying

$$L_i(X_{i_j}) = \bar{w}(X_{i_j}),\ j = 1,2,3. \tag{12}$$

6. **GREEN**. This method uses the Green's theorem in the evaluation of the average value of the gradient of a function to be recovered and was proposed in [5]. The idea of this method is based on the following approximations:

$$\nabla w|_{D_i} \approx \frac{1}{|D_i|}\int_{D_i} \nabla w\ dx = \frac{1}{|D_i|}\int_{\partial D_i} w\ n\ dx = \frac{1}{|D_i|}\sum_{j \in S(i)} \int_{\Gamma_{ij}} w\ n_{ij}\ dx.$$

For the function w on Γ_{ij} the weighted average is used

$$w|_{\Gamma_{ij}} \approx \frac{w_i|D_j| + w_j|D_i|}{|D_j| + |D_i|}. \tag{13}$$

Using the above approximations we obtain

$$\nabla w|_{D_i} \approx \frac{1}{|D_i|}\sum_{j \in S(i)} |\Gamma_{ij}| \frac{w_i|D_j| + w_j|D_i|}{|D_j| + |D_i|} n_{ij}, \tag{14}$$

This approximation of the gradient of w is then used in (6) as ∇L_i.

7. **MLS**. Using notation from the method DEO–M and Figure 2 we look for a linear function L_i which minimizes the functional

$$S(L_i) = \left(L_i(P_i) - w_i\right)^2 + \sum_{j=1}^{3} \left(L_i(P_{ij}) - w_{ij}\right)^2. \tag{15}$$

This minimization is performed by *the method of the least squares* (see Section 3.1).

2.2 Slope Limiter

To avoid spurious oscillations in the solution we use the Barth–Jesperson slope limiter from [1]. We set

$$\hat{w}_{ij}^{old} = w_i + \nabla L_i \cdot (x_i - x_{ij}, y_i - y_{ij})^T, \quad j \in S(i),\ i \in I, \tag{16}$$

and compute

$$\hat{w}_{ij} = w_i + \Phi_i \nabla L_i \cdot (x_i - x_{ij}, y_i - y_{ij})^T, \quad j \in S(i),\ i \in I, \tag{17}$$

where

$$\Phi_i = \min_{j \in S(i)} \Phi_{ij},$$

$$\Phi_{ij} = \begin{cases} 1, & \hat{w}_{ij}^{old} - w_i = 0, \\ \min(1, \frac{w_i^{max} - w_i}{\hat{w}_{ij}^{old} - w_i}), & \hat{w}_{ij} - w_i > 0, \\ \min(1, \frac{w_i^{min} - w_i}{\hat{w}_{ij}^{old} - w_i}), & \hat{w}_{ij} - w_i < 0. \end{cases} \tag{18}$$

Here $\hat{w}_{ij}^{old}$ is obtained from (16) and

$$w_i^{min} = \min(w_i, \min_{j \in S(i)} w_j), \qquad w_i^{max} = \max(w_i, \max_{j \in S(i)} w_j). \tag{19}$$

The application of the slope limiter guarantees that the following condition is satisfied

$$w_i^{min} \le \hat{w}_{ij} \le w_i^{max}, \quad j \in S(i), \ i \in I. \tag{20}$$

3 Determination of the Order of Accuracy

Let w be the exact solution of a physical problem and w_h its numerical approximation on $\mathcal{D}_h$. We suppose that

$$\|w - w_h\|_{L^p} \approx C \cdot h^{\alpha}, \tag{21}$$

where h denotes the mesh size parameter, C is a positive constant and α is called the *order of accuracy* of a scheme in L^p – norm, $(1 \le p \le \infty)$. If we know the analytical solution of the problem, we can compute the approximate solution w_h for different mesh size parameters h and using the method of the least squares to determine α and C.

3.1 Method of the Least Squares

Now we will suppose that the relation (21) holds precisely, i.e.

$$\|w - w_h\|_{L^p} = C \cdot h^{\alpha}. \tag{22}$$

We define the *error of the method* as

$$e_h \equiv \|w - w_h\|_{L^p}. \tag{23}$$

Our aim is to determine the constant C and the order of accuracy α providing the analytical solution is known. We compute the approximate solution w_h for N different meshes $(N \ge 2)$, i.e. we have $h_i, e_{h_i}, i = 1, \dots, N$. Now it is possible to use the *method of the least squares.*

From (22) and (23) we have the relation

$$e_h = C \cdot h^{\alpha}. \tag{24}$$

On (24) we apply the operator of logarithm and it leads to the relation

$$\log e_h = \log C + \alpha \cdot \log h. \tag{25}$$

If we denote

$$
\begin{aligned}
y &= \log e_h, \\
x &= \log h, \\
\beta &= \log C.
\end{aligned}
\tag{26}
$$

we get in (25) the linear dependence of y on x given by the parameters α and β. Due to the relation (21) this dependence is linear only in the sense of least squares method which leads us to the determination of α and β in such a way, that the sum

$$
S(\alpha,\beta) = \sum_{i=1}^{N} (y_i - \beta - \alpha \cdot x_i)^2 , \tag{27}
$$

where $y_i = \log e_{h_i}$, $x_i = \log h_i, i = 1, \ldots, N$, is minimal.

The conditions of the minimum of S lead to the relation for α, β

$$
\alpha = \frac{N \sum_{i=1}^{N} x_i y_i - \sum_{i=1}^{N} x_i \sum_{i=1}^{N} y_i}{N \sum_{i=1}^{N} x_i^2 - \left(\sum_{i=1}^{N} x_i\right)^2}, \tag{28}
$$

$$
\beta = \frac{\sum_{i=1}^{N} y_i - \alpha \sum_{i=1}^{N} x_i}{N}. \tag{29}
$$

Further we define the *correlation coefficient* r

$$
r = \frac{N \sum_{i=1}^{N} x_i y_i - \sum_{i=1}^{N} x_i \sum_{i=1}^{N} y_i}{\sqrt{\left(N \sum_{i=1}^{N} x_i^2 - \left(\sum_{i=1}^{N} x_i\right)\right)\left(N \sum_{i=1}^{N} y_i^2 - \left(\sum_{i=1}^{N} y_i\right)\right)}}. \tag{30}
$$

We have $r \in [-1, 1]$ and $r \approx 1$ means that the relation

$$
y_i \approx \beta + \alpha \cdot x_i, \quad i = 1, \ldots, N \tag{31}
$$

is valid almost precisely (for $r = 1$ it is valid exactly) and if $r \ll 1$ than this relation is valid inaccurately.

3.2 Sod's Channel

To determine the order of accuracy of proposed methods we have solved the Sod's channel problem (see [7])

$$
\frac{\partial}{\partial t}\begin{pmatrix} \rho \\ \rho v \\ e \end{pmatrix} + \frac{\partial}{\partial x}\begin{pmatrix} \rho v \\ \rho v^2 + p \\ (e+p)v \end{pmatrix} = 0, \qquad x \in \mathbf{R}, \tag{32}
$$

where

$$
p = (\kappa - 1)\left(e - \frac{1}{2}\rho v^2\right), \tag{33}
$$

with the initial conditions

$$
\begin{aligned}
v(x,0) &= 0, \\
\rho(x,0) &= \begin{cases} \rho_L, & x < x_0 \\ \rho_R, & x > x_0 \end{cases}, \\
p(x,0) &= \begin{cases} p_L, & x < x_0 \\ p_R, & x > x_0 \end{cases},
\end{aligned}
\tag{34}
$$

where we suppose $p_L > p_R$.

The exact analytical solution can be expressed in the following way:

$$p(x,t) = \begin{cases} p_L \quad , & x < x_0 - c_L t \\ p_L \left[1 - \frac{\kappa-1}{\kappa+1}\left(1 + \frac{x-x_0}{c_L t}\right)\right]^{\frac{2\kappa}{\kappa-1}}, & x_0 - c_L t < x < x_1 \\ p_2, & x_1 < x < x_o + v_c t \\ p_2, & x_0 + v_c t < x < x_0 + v_s t \\ p_R, & x > x_0 + v_s t \end{cases}, \tag{35}$$

$$v(x,t) = \begin{cases} 0, & x < x_0 - c_L t \\ \frac{2}{\kappa+1}\left(\frac{x-x_0}{t} + c_l\right), & x_0 - c_L t < x < x_1 \\ v_c, & x_1 < x < x_o + v_c t \\ v_c, & x_0 + v_c t < x < x_0 + v_s t \\ 0, & x > x_0 + v_s t \end{cases}, \tag{36}$$

$$\rho(x,t) = \begin{cases} \rho_L, & x < x_0 - c_L t \\ \rho_L \left[1 - \frac{\kappa-1}{\kappa+1}\left(1 + \frac{x-x_0}{c_L t}\right)\right]^{\frac{2}{\kappa-1}}, & x_0 - c_L t < x < x_1 \\ \rho_L \left(\frac{p_2}{p_L}\right)^{\frac{1}{\kappa}}, & x_1 < x < x_o + v_c t \\ \rho_R \frac{1 + \frac{\kappa+1}{\kappa-1}\frac{p_2}{p_R}}{\frac{\kappa+1}{\kappa-1} + \frac{p_2}{p_R}}, & x_0 + v_c t < x < x_0 + v_s t \\ \rho_R, & x > x_0 + v_s t \end{cases}. \tag{37}$$

Here

$$x_1 = x_0 + \left(\frac{\kappa+1}{2} v_c - c_L\right) t, \tag{38}$$

for the speed of the *shock wave* v_s we have

$$v_s = c_R^2 \frac{\frac{p_2}{p_R} - 1}{\kappa v_c} \tag{39}$$

and for the speed of *contact discontinuity* it holds

$$v_c = c_R \sqrt{\frac{2}{\kappa(\kappa-1)}} \frac{\frac{p_2}{p_R} - 1}{\sqrt{1 + \frac{\kappa+1}{\kappa-1}\frac{p_2}{p_R}}}. \tag{40}$$

Moreover the pressure p_2 has to be determined. For p_2 one can find the following equation

$$\sqrt{\frac{2}{\kappa(\kappa-1)}} \frac{\frac{p_2}{p_R} - 1}{\sqrt{1 + \frac{\kappa+1}{\kappa-1}\frac{p_2}{p_R}}} = \frac{2}{\kappa-1}\frac{c_L}{c_R}\left[1 - \left(\frac{p_2}{p_L}\right)^{\frac{\kappa-1}{2\kappa}}\right], \tag{41}$$

which can be solved numerically. The local speed of sound c_L and c_R are obtained from the initial conditions.

The analytical solution of the problem (32) – (34) is demonstrated for the density in Figure 3. The contact discontinuity (between regions 3 and 2) and the shock wave (between regions 2 and R) propagate in the positive direction of the axis x from the point $(x_0, 0)$ with speed v_c and v_s, respectively. The expansion region (region 4) increases in the negative direction of the axis x, its edges propagate with the speed c_L and $(\kappa+1)v_c/2 - c_L$, respectively. In regions L and R, there are constant values given by initial conditions. The Figure 4 shows 3-D plot of the density in the (x,t) plane.

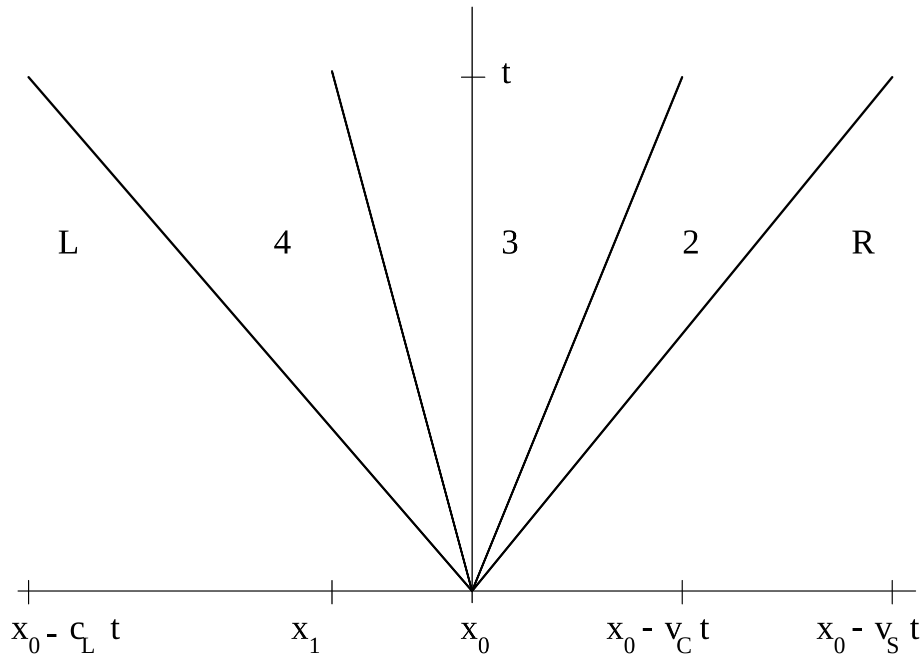

Figure 3: Propagation of discontinuities for Sod's channel

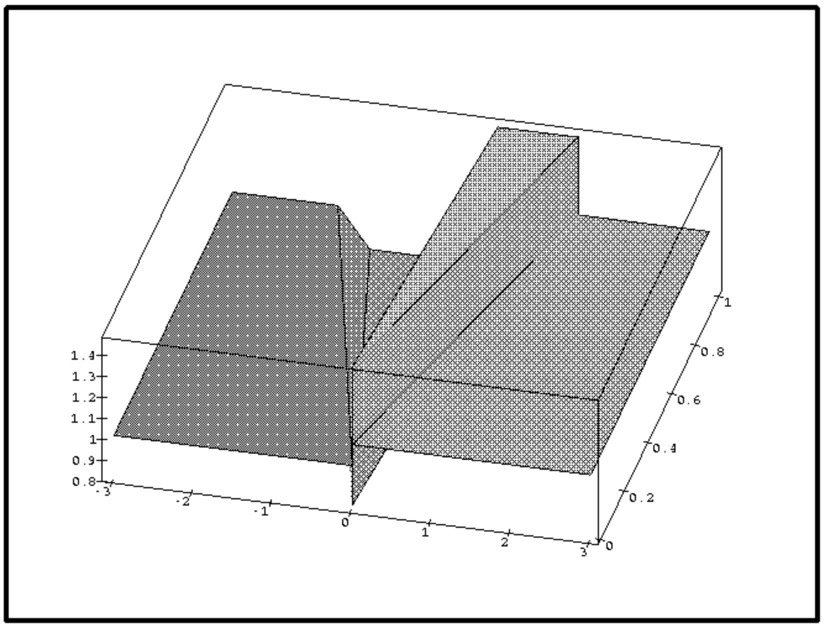

Figure 4: Density distribution in (x, t) plane

4 Numerical Results

To determine the order of accuracy of our schemes we solved the Sod's channel problem in the domain $\Omega = [-3:3] \times [0:0.1]$ using the 2D code described in [4] for the numerical solution of the Euler equations (1) equipped by the initial conditions (34), where

$$\begin{aligned} \rho_L &= 1.00, & p_L &= 2.00, \\ \rho_R &= 1.101463, & p_R &= 1.00. \end{aligned} \tag{42}$$

The analytical and approximate solution are computed at time $t = 1$. We have used three triangulations containing 75×4, 150×8 and 300×16 nodes, respectively, computed the error $e_h = \|\rho - \rho_h\|_{L^1(\Sigma)}$ and using the method of the least squares we determined the order of accuracy α and the constant C. For the domain Σ where we investigate the order of accuracy, two cases were distinguished

1. **whole** – we put $\Sigma = \Omega$
2. **smooth** – we put $\Sigma = \Omega - \sigma$, where $\sigma \subset \Omega$ is a "narrow corridor" along discontinuities, i.e. Σ is a subdomain of Ω where the solution u is smooth.

The results are in the following table (α is the order of accuracy, C the constant from (22) and r the correlation coefficient defined by (30).

			whole			smooth	
num.	method	α	C	r	α	C	r
0.	BASIC	0.627	0.065	0.999	1.062	0.106	0.999
1.	DEO–M	0.210	0.021	0.981	0.074	0.009	0.546
2.	DEO–B	0.203	0.016	0.630	0.010	0.004	0.019
3.	MIN	0.848	0.063	0.991	1.399	0.094	0.987
4.	AVER	- 0.222	0.008	-0.757	- 0.298	0.005	-0.794
5.	EXTRAP	-0.032	0.009	-0.520	-0.375	0.002	-0.915
6.	GREEN	0.599	0.061	0.999	1.022	0.097	0.999
7.	MLS	0.594	0.044	0.998	1.270	0.113	0.999

We can see from the table that in the second case only 3 methods give reasonable results: MIN, GREEN and MLS. The method GREEN gives results corresponding to the first order and only methods MIN and MLS bring some increasing of order of accuracy. The best one seems to be MIN. On the other hand the scheme is not a second order one. Figures 5, 6 and 7 show the comparison of analytical solution (dashed line), numerical solution obtained by the basic scheme (pointed line) and numerical solution obtained by MIN (full line) for three different meshes.

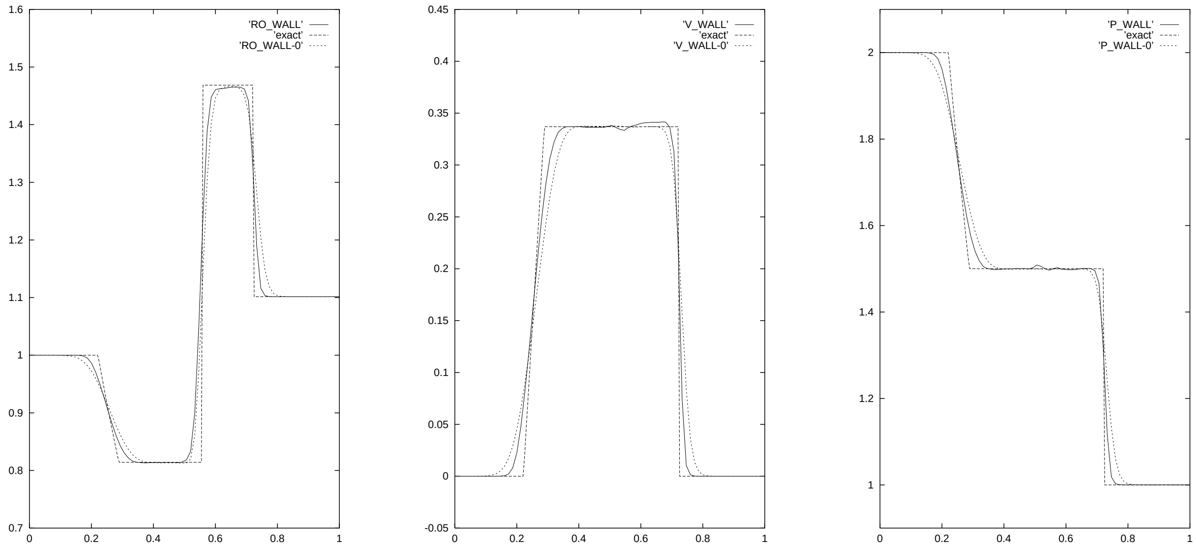

Figure 5: Distribution of density, velocity and pressure for Sod's channel on mesh 75×4 nodes

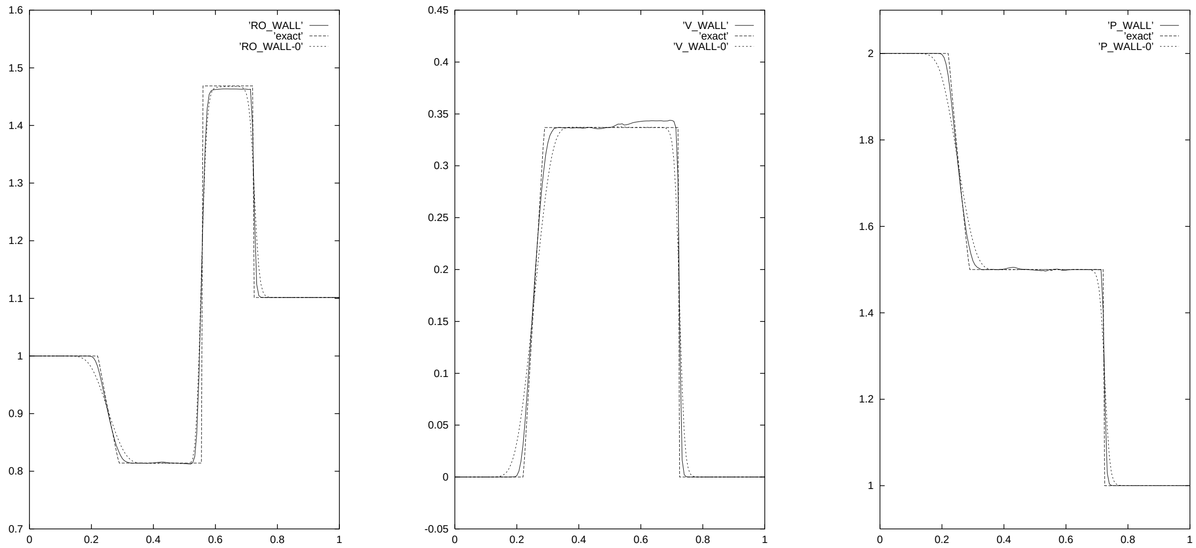

Figure 6: Distribution of density, velocity and pressure for Sod's channel on mesh 150×8 nodes

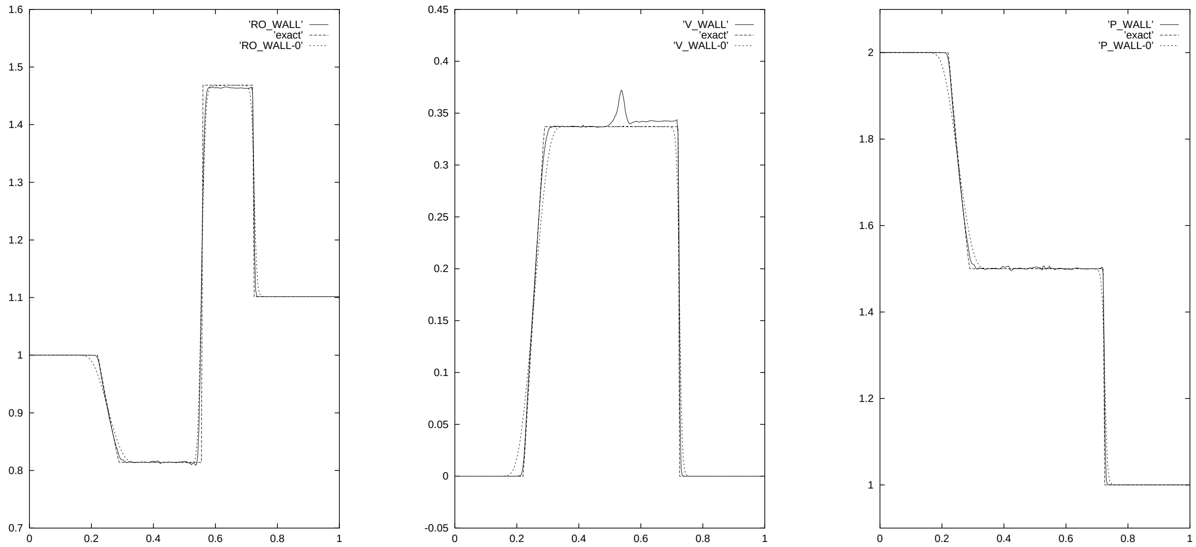

Figure 7: Distribution of density, velocity and pressure for Sod's channel on mesh 300×16 nodes

References

[1] T. J. Barth and D. C. Jespersen. The design and application of upwind schemes on unstructured meshes. *AIAA Journal*, 366, 1989.

[2] L. J. Durlofsky, B. Enquist, and S. Osher. Triangle based adaptive stencils for the solution of hyperbolic conservation laws. *Journal of Computational Physics*, 98:64–73, 1992.

[3] Miloslav Feistauer. *Mathematical Methods in Fluid Dynamics.* Longman Scientific & Technical, Harlow, 1993.

[4] M. Feistauer, J. Felcman, M. Lukáčová–Medviďová. *Combined finite element–finite volume solution of compressible flow.* J. Comput. Appl. Math. 63 (1995), 179–199.

[5] L. Flandrin, P. Charrier, and B. Dubroca. A robust finite volume method for computations of two-dimensional unstructured hybrid meshes. In S. Wagner, E. H. Hirschel, J. Périaux, and R. Piva, editors, *Computational Fluid Dynamics '94*, pages 301–308, ISBN 0-471-950637, 1994. John Wiley and Sons, Stuttgart.

[6] S. Osher and F. Solomon. Upwind difference schemes for hyperbolic systems of conservation laws. *Math. Com.*, 38:339–374, 1982.

[7] G. A. Sod. A survey of several finite difference methods for system of nonlinear hyperbolic conservation laws. *Journal of Computational Physics*, 27:1–31, 1978.